JOURNAL OF MATERIALS SCIENCE **36** (2001) 2417–2426

Material characterisation and mechanical properties of Al_2O_3-Al metal matrix composites

B. G. PARK
Tohoku National Industrial Research Institute, 4-2-1 Nigatake, Miyagino-ku, Sendai, Japan 938-8551

A. G. CROSKY
School of Materials Science and Engineering, The University of New South Wales, Sydney 2052, Australia

A. K. HELLIER
Materials Division, Australian Nuclear Science and Technology Organisation, Private Mail Bag 1, Menai, NSW 2234, Australia
E-mail: akh@ansto.gov.au

The mechanical properties of metal matrix composites (MMCs) are critical to their potential application as structural materials. A systematic examination of the effect of particulate volume fraction on the mechanical properties of an Al_2O_3-Al MMC has been undertaken. The material used was a powder metallurgy processed AA 6061 matrix alloy reinforced with MICRAL-20^{TM}, a polycrystalline microsphere reinforcement consisting of a mixture of alumina and mullite. The volume fraction of the reinforcement was varied systematically from 5 to 30% in 5% intervals. The powder metallurgy composites were extruded then heat treated to the T6 condition. Extruded liquid metallurgy processed AA 6061 was used to establish the properties of the unreinforced material.

1. Introduction

The main purpose for producing metal matrix composites (MMCs) is to achieve light materials with high specific strength and stiffness. Of special interest in this regard are particulate reinforced metal matrix composites (PRMMCs), which possess several additional advantages. Firstly, they offer cost effective manufacturing; particulate forms of reinforcement are much cheaper than long fibres. PRMMCs can also be manufactured by conventional metallurgical processes, and secondary processing can be applied. Secondly, PRMMCs have isotropic properties (not the case for continuously reinforced MMCs). Therefore, they can be used for more general applications. Thirdly, they can be produced in large quantities as is required for structural applications.

The intrinsic advantage of MMCs over the unreinforced alloy is the improvement of mechanical properties due to addition of the reinforcing material. Mechanical properties of MMCs are directly related to their microstructural features such as the reinforcement, matrix/reinforcement interfaces, dislocations, etc. Generally MMCs exhibit considerable increases in strength and stiffness. However, they also have poor ductility, low values of fracture toughness and poor low-cycle fatigue properties [1–3].

The main contribution to the increase in mechanical properties of PRMMCs is particle addition; it affects most of the properties of PRMMCs. Parameters related to the particles are volume fraction, size, shape and distribution of particles, the most important parameter being the volume fraction. Lloyd [4] reported that the dominant factor in controlling the elastic modulus is the volume fraction of particles, and that it is relatively insensitive to the particle size and distribution. Moreover, as the volume fraction of particles is increased, tensile and yield strengths generally increase, and ductility and fracture toughness decrease [5–7].

The amount of thermal residual stress also depends on the volume fraction. Increasing the volume fraction monotonically increases the thermal residual stress and also increases dislocation densities [8, 9].

Grain and sub-grain sizes are smaller in the composite than in the unreinforced alloy. Arsenault [10] showed that as the particle volume fraction was increased, the dislocation density became higher and sub-grain size became smaller.

In this study, the effect of particle volume fraction on the mechanical properties of PRMMCs was examined.

2. Experimental procedure

The material used was AA 6061 alloy reinforced with MICRAL-20^{TM}, a polycrystalline 20 μm (nominal) diameter microsphere reinforcement consisting of a mixture of mullite ($Al_6Si_2O_{13}$) and alumina (α-Al_2O_3) in the ratio 68 : 32 (wt%), with the grains of each phase being typically less than 0.5 μm in size. The volume

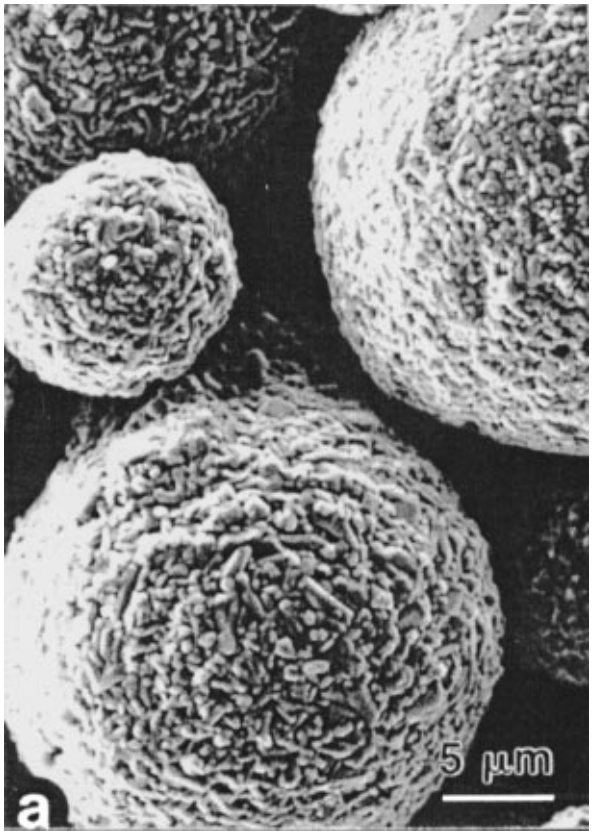

Figure 1 The original form of MICRAL-20^{TM} prior to blending [12].

fraction was varied systematically from 5 to 30% in 5% intervals. Physical and mechanical properties of MICRAL-20^{TM} are given in Table I [11]. The typical appearance of MICRAL-20^{TM} prior to blending is shown in Fig. 1 [12]. The composites were manufactured by a conventional powder metallurgy process.

Metal powder and microspheres were blended, compacted by cold isostatic pressing, and then sintered into a 125 mm diameter × 357 mm billet. The unreinforced alloy was melted and cast into a mould 125 mm diameter × 149 mm in size. All were extruded into 19 mm diameter rod. Prior to extrusion, the dies and billets (or ingot) were preheated to ∼480°C and the material then extruded at a speed of 8–10 m per minute. A liquid metallurgy composite containing 20% volume fraction of MICRAL-20^{TM}, prepared as above and designated COMRAL-85^{TM}, was also examined [13]. Discussion of the results for this material, however, lies outside the scope of the present paper.

The designation and chemical compositions of the AA 6061 and powder metallurgy composites are shown in Table II. The Mg content of the unreinforced alloy used as a reference material was at the lower end of the nominal composition range for AA 6061 (0.8–1.2 wt%). The composites also had Mg contents at the lower end of the composition range for AA 6061, except for PM 5 and PM 10, which had Mg contents slightly below the nominal range. Other elements were all within their nominal composition ranges.

Basic heat treatment cycles included a solution treatment at 530°C for 90 minutes, direct quenching into cold water, pre-aging for 20 hours at room temperature and then artificial aging at 175°C. For a typical peak aged condition for AA 6061 (heat treatment designation T6) samples were artificially aged for 8 hours. In the case of the composites, the same heat treatment cycle was followed except for the artificial aging time which was modified to 6 hours at 175°C for the peak aged condition.

After heat treatment, all specimens were subjected to a hardness test to confirm their precipitation hardening behaviour and to set up the specimen hardness database. Hardness tests, carried out on polished surfaces of specimens, were made using a Vickers hardness testing machine with a 5 kg load and 20 seconds indentation time. The diagonal length of the indentation mark was about 200 μm and tens of particles were included within the indent. The peak aged condition was deduced from graphs of hardness versus aging time. At least ten measurements were made on each specimen in order to obtain averaged hardness values.

Volume fractions of particles were measured in the polished surfaces of the composites using a Quantimet 500 image analyser fitted to an optical microscope.

The dynamic elastic modulus was measured using the Grindo-sonic method [14] for material in both the as-extruded and T6 conditions for the unreinforced alloy and composites. The measurements were made using 17 mm diameter × 170 mm specimens.

TABLE I Properties of MICRAL-20^{TM} [11]

Microsphere	E (GPa)	K_{Ic} (MPa$\sqrt{m}$)	Hardness (HV)	CTE (10^{-6} °C^{-1})	Density (g/cm^3)	Porosity (%)
MICRAL-20^{TM}	240	2.9	1140	6.3	3.4	<1

TABLE II Chemical composition of materials (wt %)

Material	V_f	Mg	Si	Cu	Fe	Mn	Cr	Ti	Al
AA 6061	0%	0.8	0.4	0.1	0.2	0.09	0.06	0.03	Balance
PM 5	5%	0.6	0.46	0.23	0.16	≤0.02	≤0.02	≤0.02	
PM 10	10%	0.7	0.52	0.25	0.18	≤0.02	≤0.02	≤0.02	
PM 15	15%	0.8	0.50	0.23	0.18	≤0.02	≤0.02	≤0.02	
PM 20	20%	0.8	0.48	0.23	0.19	≤0.02	≤0.02	≤0.02	
PM 25	25%	0.8	0.51	0.22	0.20	≤0.02	≤0.02	≤0.02	
PM 30	30%	0.8	0.48	0.22	0.22	≤0.02	≤0.02	≤0.02	

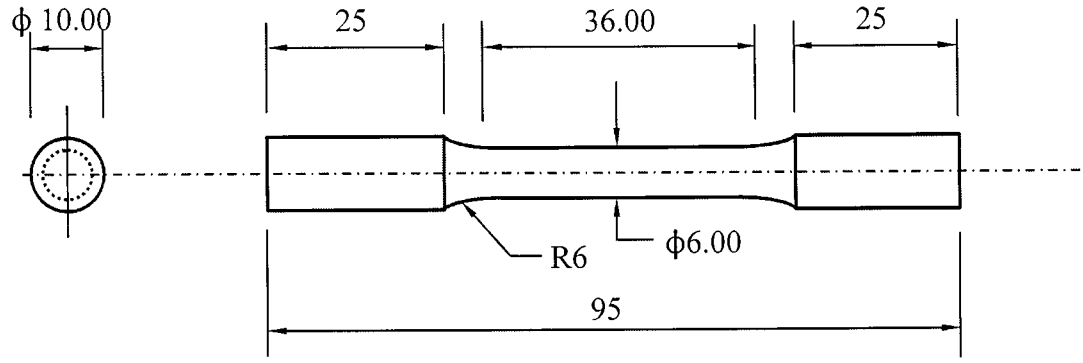

Figure 2 Schematic drawing of tensile specimen (dimensions in mm).

Tensile testing was performed in accordance with ASTM E8 under displacement control using an Instron 1185 100 kN screw-driven machine. The crosshead speed was 0.2 mm/min, giving a strain rate of 10^{-4} sec^{-1} for the specimen gauge length used. Test specimens were machined from the as-extruded bar with the loading axis parallel to the extrusion direction. For testing materials in the T6 condition, the specimens were heat treated prior to machining to prevent specimen distortion by thermal residual stress. Because of the limited available material, reduced size specimens were used with a gauge length of 36 mm and an approximate cross-sectional area of 28.3 mm^2, as shown in Fig. 2. Specimen strain was monitored using an extensometer with a gauge length of 25 mm. Three specimens were tested for each material.

After tensile testing the fractured specimens were metallographically sectioned longitudinally. The number of particles which were present on the fracture surface was counted manually. Debonded particles were weighted by a factor of two when obtaining the total particle count, since only 50% of the debonded particles should be present on either of the two mating fracture surfaces. The results were then compared with the number of particles present along an arbitrary straight path of the same length as the projected fracture surface. This value was obtained by counting the particles along five randomly selected straight lines parallel to the fracture surface and then averaging the results.

Optical microscopy was used to examine microstructure and particle size distribution. Specimen preparation procedures for optical microscopy included several steps of grinding and polishing. Material was sectioned by a low speed diamond saw both in the longitudinal and transverse direction. The sectioned material was then mounted and ground using SiC grinding paper. Polishing was carried out using 3 μm and 1 μm diamond paste. Final polishing was carried out on a rubber pad using colloidal silica which was a suspension of 0.05 μm SiO_2 particles.

A JEOL 840 scanning electron microscope (SEM) was used to examine fracture surfaces of the specimens after tensile testing. Standard preparation and imaging procedures were used. The specimens were given a coating of carbon and examined using an accelerating voltage of 20 kV.

3. Results

3.1. Aging response

Aging curves for the composites at 175°C are shown in Fig. 3. The aging response was generally similar for all six of the composites with the hardness increasing progressively with volume fraction. Peak hardness was achieved in 6 hours and this time was therefore used as the T6 aging time for all the composites.

The particle volume fraction was measured using an image analyser for each of the composites from samples cut from the tensile specimens. The results are given in Table III. The measured volume fractions are close to the nominal values.

3.2. Microstructure

A longitudinal section of a sample containing 20% volume fraction of particles (designated PM 20) is shown in Fig. 4, from which it is apparent that the composite shows little evidence of particle clustering. Damaged particles were frequently observed in the composites at the higher volume fractions but to a much lesser extent

TABLE III Measured particle volume fractions

Materials	PM 5	PM 10	PM 15	PM 20	PM 25	PM 30
Nominal V_f	5%	10%	15%	20%	25%	30%
Measured V_f	5.6%	9.2%	14.1%	19.7%	24.6%	28.9%

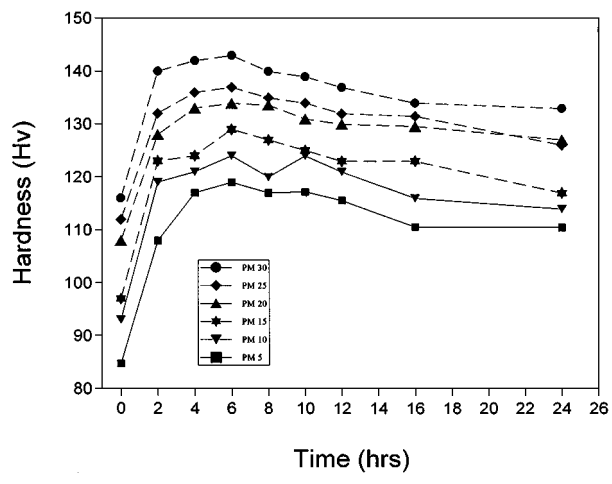

Figure 3 Aging response of composites.

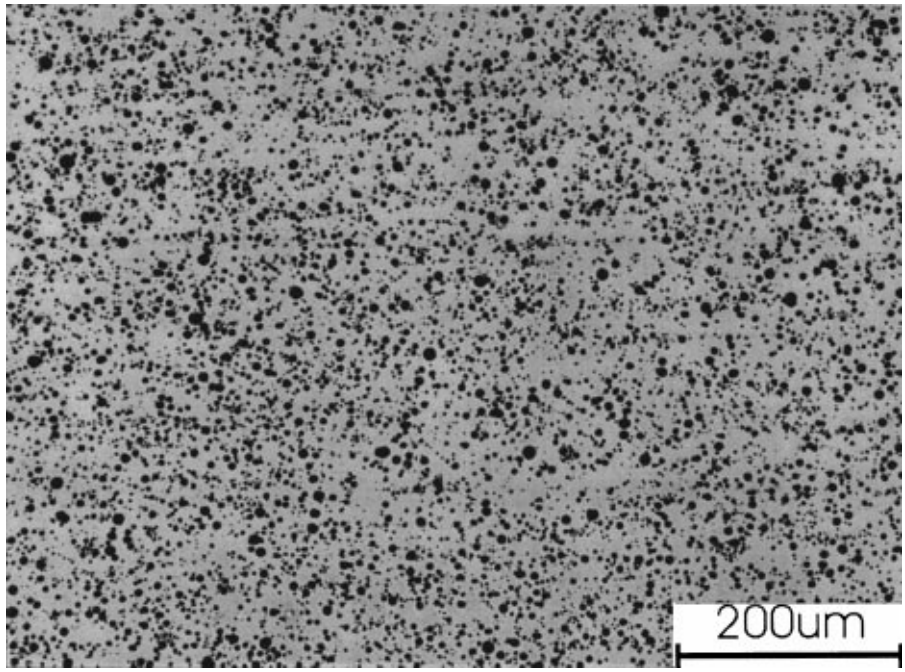

Figure 4 Optical micrograph of PM 20 at low magnification.

at the lower volume fractions. In the high volume fraction (25% and 30%) composites, regions in which a small number of particles were in contact were frequently observed, Fig. 5, and micro-porosity was seen to occur in between the particles in these regions. For the lower volume fractions, particle contact was rare and no pores were detected in the material, even when examined at magnifications up to 500×.

3.3. Mechanical properties

3.3.1. Elastic modulus

The elastic moduli of the unreinforced matrix alloy and the six composites are shown in Fig. 6. The elastic modulus increased with increasing volume fraction of particulate, but the rate of increase in the modulus decreased slightly with increasing volume fraction.

3.3.2. Hardness

The hardness of the composites is shown as a function of particle volume fraction in Fig. 7. Data is given for the material before heat treatment (i.e., as-extruded) as well as for the T6 condition. The results show that the hardness varies linearly with volume fraction in both the T6 and as-extruded conditions. However, the effect is about 40% greater for the material in the T6 condition than for the as-extruded material, with the rates of increase being 1.05 and 0.75 HV per 1% particle addition respectively.

3.3.3. Tensile properties

The tensile properties are shown as a function of volume fraction for the T6 condition in Fig. 8. For each material three specimens were used to obtain the results. The addition of particulate significantly increases both yield (0.2% proof strength) and tensile strength, but the effect does not increase with increasing volume fraction. On the contrary, the results suggest that the yield and tensile strengths both decrease slightly as the volume fraction of particulate is increased. Results were also obtained from material in the as-extruded condition. In this condition, the yield and tensile strengths were not increased markedly by the addition of particulate, Fig. 9, although a general increase occurred with increase in volume fraction. The ductility decreased linearly with particle volume fraction in both the as-extruded and T6 conditions, Fig. 10.

3.3.4. Fractography

Fracture surfaces of the composites are shown in Fig. 11 and Fig. 12 for the T6 and as-extruded conditions respectively. In the T6 condition, fractured particles are clearly seen on the fracture surface while fractured particles are less frequently observed in the as-extruded condition. This observation was supported by quantitative analysis of the crack profiles, Fig. 13, which shows that more fractured particles are associated with the crack profile in the T6 condition than in the as-extruded condition. The results also show that there are more particles (fractured plus unfractured) on the fracture surface than on an arbitrary parallel section, indicating that the fracture exploits the particles.

4. Discussion

4.1. Aging response

The aging process in AA 6061 consists of several steps: supersaturated solid solution → Si-vacancy clusters → spherical G. P. zones → β'' needles → β' rods → equilibrium β-Mg_2Si plates [15]. When aging is carried out below the critical $\beta'' \rightarrow \beta'$ transformation temperature (∼200°C), as was the case in this work where the aging temperature was 175°C, the main

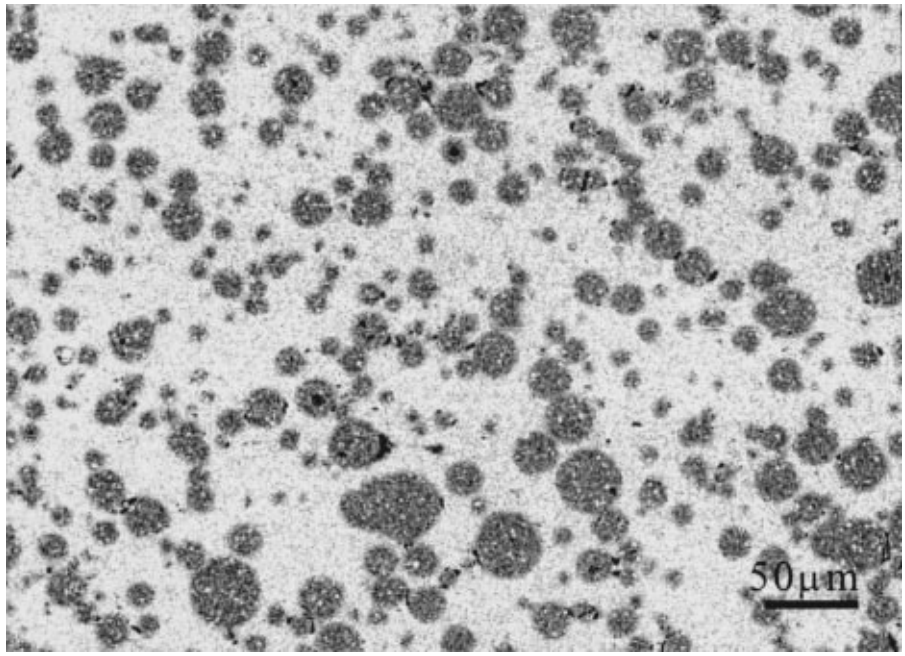

(a)

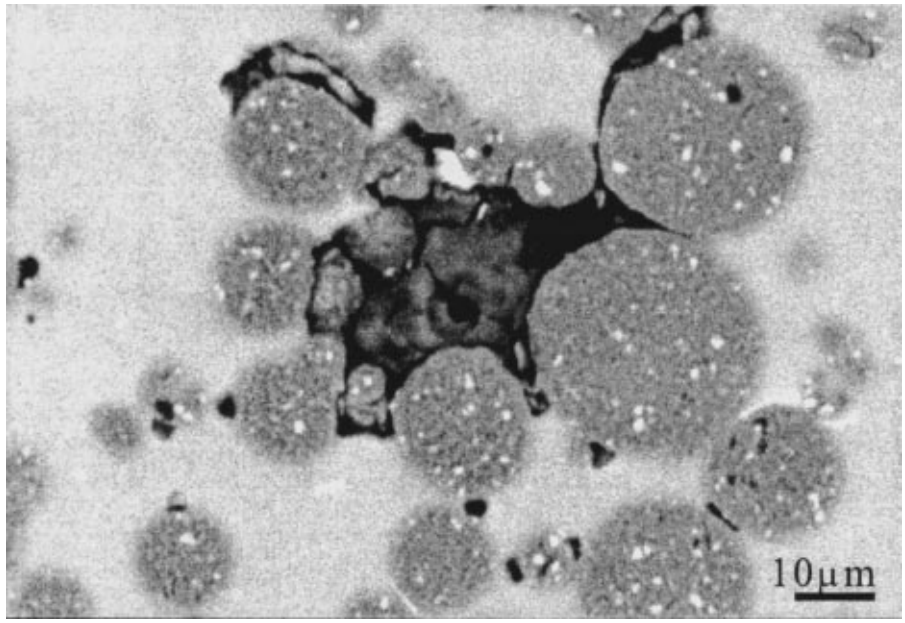

(b)

Figure 5 SEM micrographs of PM 30 showing broken particles and voids formed in a particle cluster.

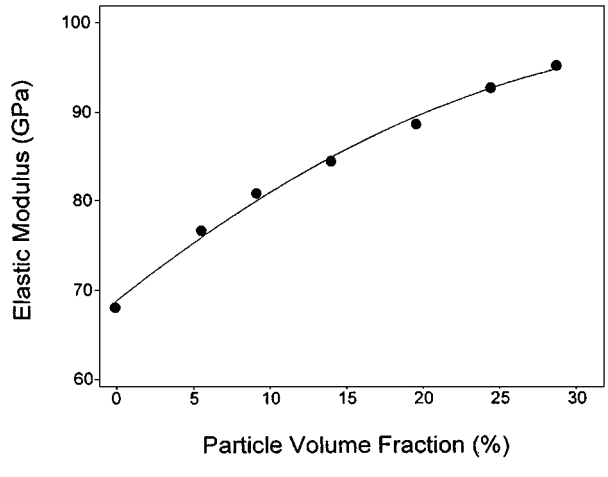

Figure 6 Elastic modulus versus particle volume fraction.

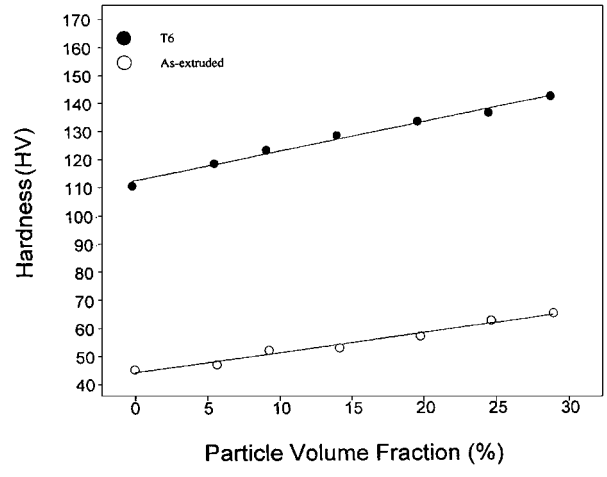

Figure 7 Hardness values of composites in the T6 and as-extruded conditions.

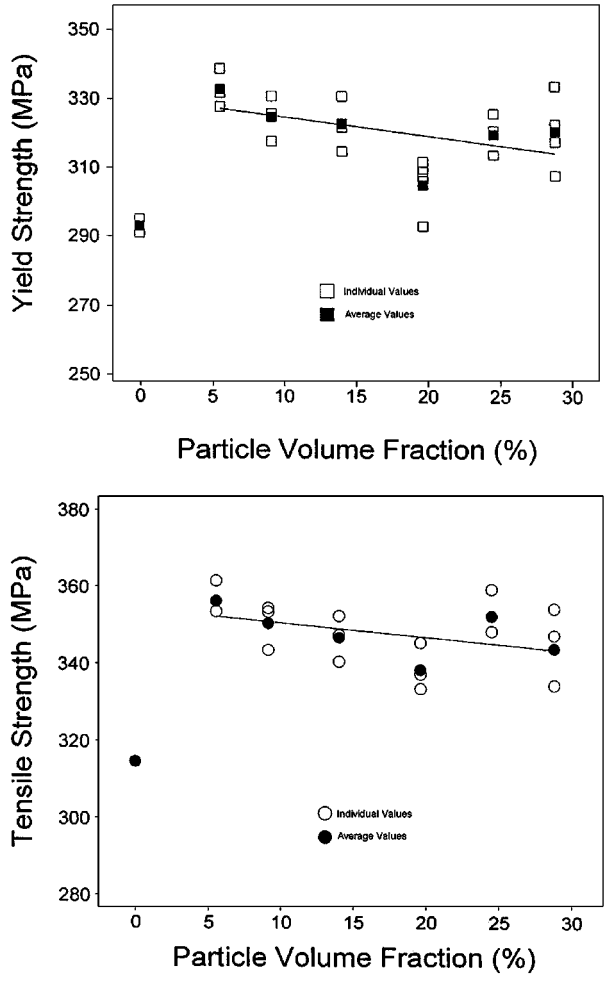

Figure 8 Yield strength and tensile strength of composites in the T6 condition.

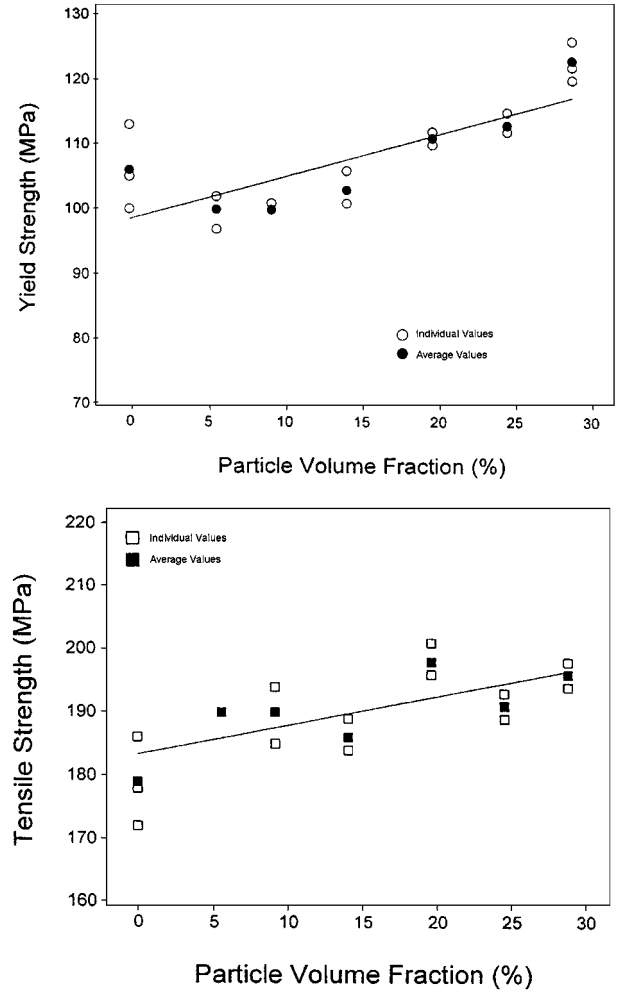

Figure 9 Yield strength and tensile strength of composites in the as-extruded condition.

strengthening phase is the needle shaped β''. It is generally accepted that particle addition does not alter the aging sequence but accelerates the aging kinetics of the strengthening precipitates. High dislocation densities are produced by the addition of particles as a result of the difference in the coefficient of thermal expansion (CTE) of the particles and the matrix. This difference is substantial for MICRAL-20^{TM} reinforced AA 6061 for which the values are $6.3 \times 10^{-6}\,^{\circ}C^{-1}$ [11] and $24 \times 10^{-6}\,^{\circ}C^{-1}$ [16] respectively. The high dislocation densities, and also the particle/matrix interfaces, provide short circuit diffusion paths which accelerate the aging process. However, the dislocations and interfaces also provide sinks for quenched-in vacancies, and this can retard nucleation.

The powder metallurgy processed composites showed an acceleration in the aging response (i.e., the time to attain peak hardness). This is supported by previous work on AA 6061 which has shown that the formation of the intermediate phase, β'', occurs faster in powder metallurgy material than in the liquid metallurgy processed alloy [17].

It is of interest to note that the aging response of the composites was not affected by the particulate volume fraction. A similar result was obtained by Dionne and Lo [18] for powder metallurgy processed AA 6061 containing 25 and 30 volume % SiC particulate. As in the present study, Dionne and Lo [18] found that the aging kinetics were faster in the powder metallurgy composites than in the matrix alloy.

4.2. Elastic modulus

The results show that the addition of particulate increases the elastic modulus, the effect becoming greater with increasing volume fraction. The experimental data is compared with the values predicted by a number of models [19–23] in Fig. 14. The predicted values were calculated using the measured modulus of the matrix alloy, the measured volume fractions and the reported modulus of the MICRAL-20^{TM} reinforcement [11].

The results show reasonable agreement with the Ge and Schmauder model [21] at low volume fractions but exhibit an increasing deviation from this model as the volume fraction increases. Metallographic examination revealed that broken particles were present in the composites and that the level of particle fracture increased with volume fraction. Elomari *et al.* [24] have shown that particle fracture reduces the elastic modulus in AA 6061 reinforced with alumina particles, and the same would be expected for the composite studied here. Since the level of particle fracture increased with volume fraction, an increasing deviation from linear behaviour would be expected and this may account for

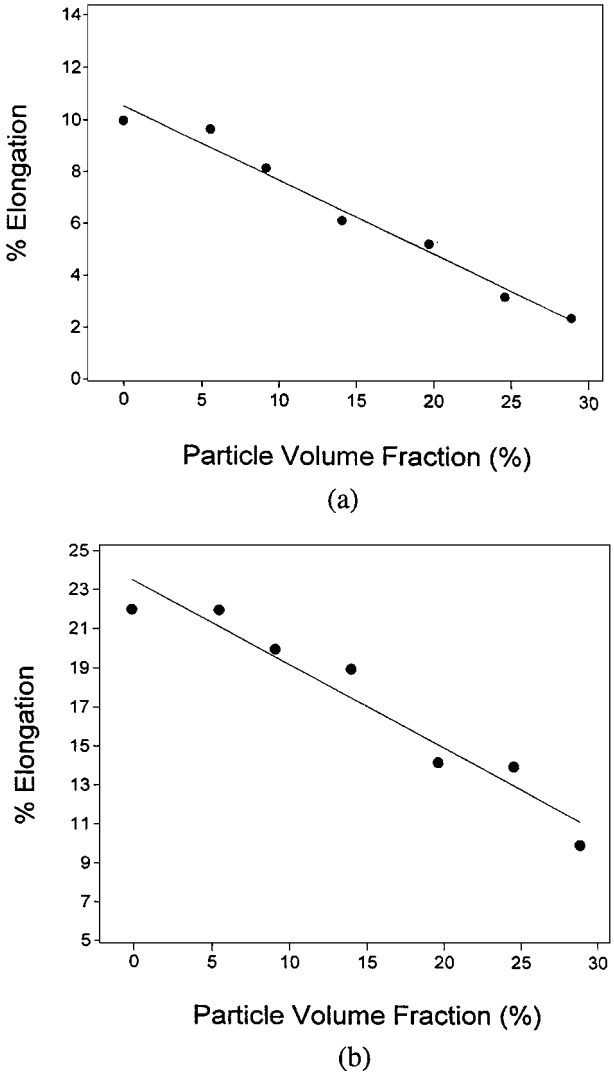

Figure 10 Percent elongation of composites, (a) in the T6 condition, and (b) in the as-extruded condition.

the increasing deviation from the Ge and Schmauder model as the volume fraction increases.

4.3. Hardness

The hardness of the composites increased progressively with volume fraction, with the results indicating that the rate of increase was linear, Fig. 7. The increase in hardness produced by the addition of particulate is consistent with the view that the particulate strengthens the composites. There are a number of factors which contribute to the strengthening effect including residual elastic stresses, increased dislocation densities, decreased grain and subgrain size and increased plastic constraint. The relative contributions from these various effects cannot be established from the results of this study, but it is apparent that their combined effect increases linearly with volume fraction. Certainly, the dislocation density, residual stresses and the level of plastic constraint would be expected to increase progressively with volume fraction. It would also be expected that the increasing dislocation density would improve the aging response of the matrix, as is found in material cold-worked before aging, and that this would

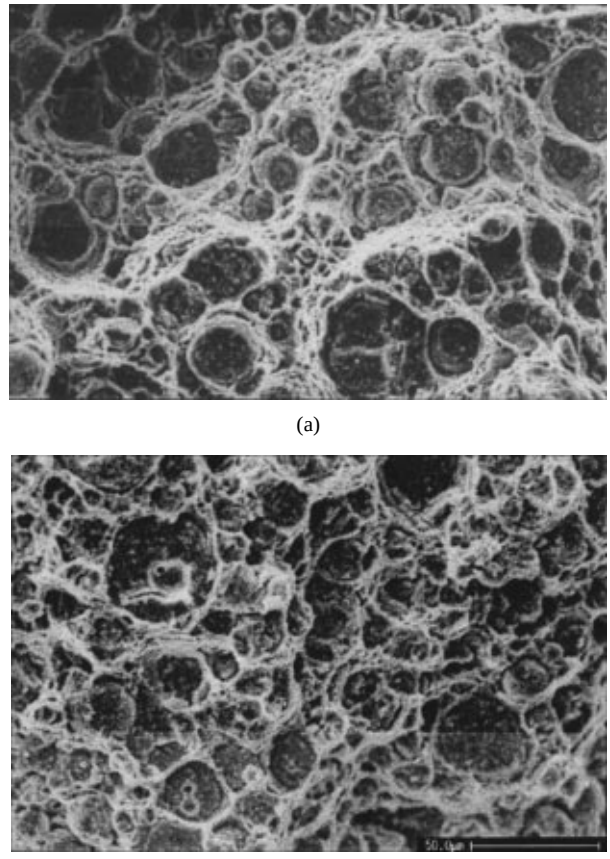

Figure 11 SEM micrographs of fracture surfaces of composites in the T6 condition with, (a) 15% particulate, and (b) 30% particulate.

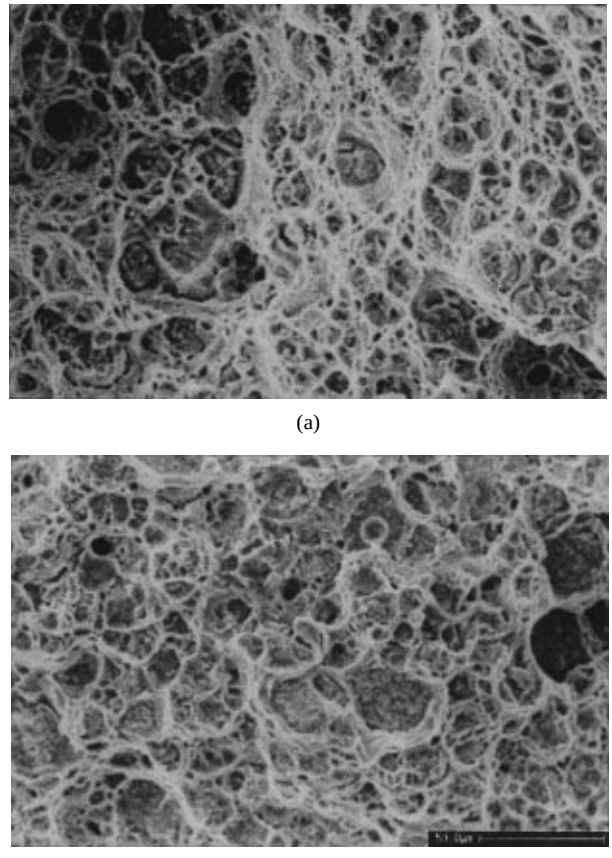

Figure 12 SEM micrographs of fracture surfaces of composites in the as-extruded condition with, (a) 15% particulate, and (b) 30% particulate.

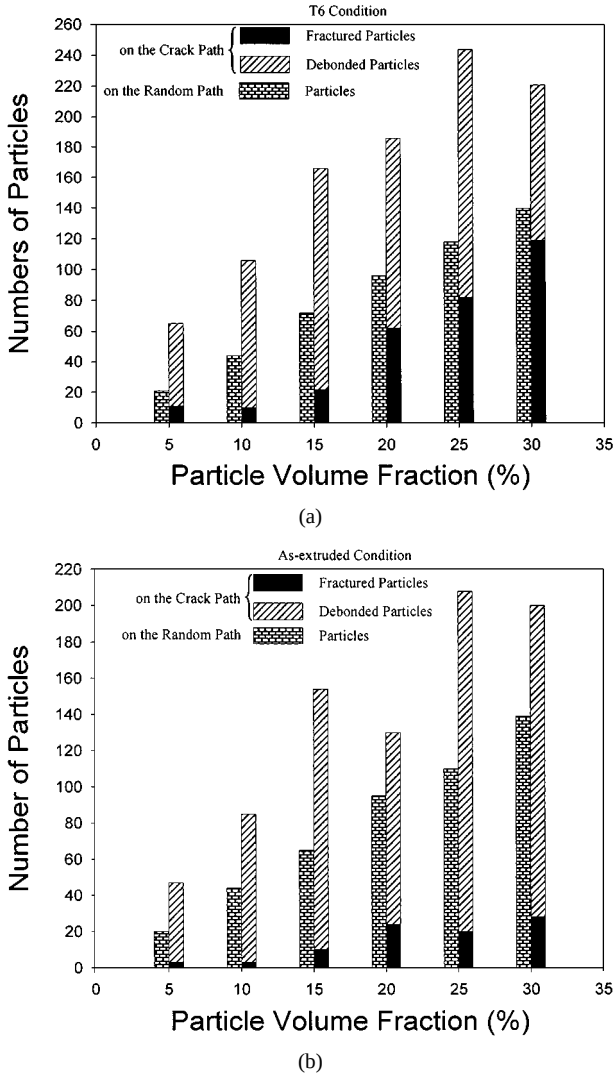

Figure 13 Comparison of number of particles encountered on a random path with number observed on crack path, (a) in the T6 condition, and (b) in the as-extruded condition.

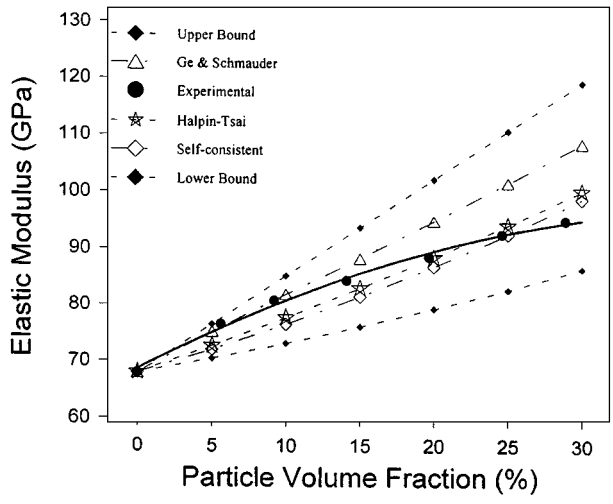

Figure 14 Comparison of measured elastic moduli with moduli predicted using upper [19] and lower bound [20], Ge & Schmauder [21], Halpin-Tsai [22] and self-consistent [23] models. The aspect ratio used in the Halpin-Tsai model was 1.0 and the Poisson's ratio used in the Ge & Schmauder model was 0.33.

produce an additional progressive increase due to increasing matrix strength. This is consistent with the finding that hardness increased more rapidly with volume fraction for the composites in the T6 condition than in the unhardened as-extruded condition.

It is interesting to note that the aging kinetics were not affected by increasing the volume fraction of particles and this would, at first sight, suggest that the dislocation density did not increase with increasing volume fraction. However, as discussed earlier, an alternative explanation for the observed aging behaviour could be that the acceleration in kinetics which would result from the increased density of dislocations was offset by a retardation due to annihilation of quenched-in vacancies by the dislocations, and this would then be consistent with the increase in hardness being at least in part due to an increase in dislocation density.

Crawford and Griffiths [25] have conducted hardness and tensile tests on MICRAL-20^{TM} reinforced AA 6061 composites with the same nominal volume fractions as in the present work, and heat treated to the T6 condition (aging was at 175°C for 8 hours rather than the 6 hours used here). Their microhardness results show a systematic increase of approximately 6% (from 132 HV to 140 HV) as the volume fraction increases from 5% to 30%. Comparison with Fig. 7 shows that these data are consistent with the present results. Crawford and Griffiths assume that this slight increase may be caused by increased plastic constraint as the particle spacing decreases and conclude that the yield stresses of the various composites were effectively constant.

4.4. Tensile properties

While the hardness of the composites increased progressively with volume fraction the strength did not, at least for the material age hardened to the T6 condition. The addition of 5% particulate produced an initial increase in both the yield strength (0.2% proof stress) and tensile strength to about 10% above that of the unreinforced alloy, but further addition of particulate produced no further increase in strength. Instead, a slight progressive reduction in both yield and tensile strength was observed, Figs 8 and 9. The hardness results clearly indicate that the addition of particulate produces a progressive strengthening effect, and progressive increases with increasing volume fraction would thus be expected in the yield and tensile strengths. However, similar effects have been reported elsewhere. Ravi Kumar and Dwarakadasa [26] observed lower yield and tensile strengths in Al-Zn-Mg composite than in the unreinforced alloy, which Dionne *et al.* [27] interpreted as being due to premature fracture of the particles during loading. Indeed, in their work on SiC/7091, Dionne *et al.* confirmed that particle fracture occurred before the ultimate strength of the matrix was reached. To account for the reduction in yield strength as well as tensile strength, particle fracture would have to occur at stresses below that at which the matrix yields.

Fractographic results show that particle fracture does occur in the age hardened composites, and that it occurs well ahead of the crack tip, and thus at stresses

substantially below the ultimate strength of the matrix. In view of these findings it appears that the observed behaviour can be explained by two competing effects. As the volume fraction of particulate increases, strengthening occurs due to matrix strengthening from increased dislocation density and increased aging response. However, during tensile loading, particle fracture occurs below the yield strength of the matrix, so that the load is carried only by the matrix. As the volume fraction increases, the amount of matrix remaining to carry the load decreases so that final failure occurs at a lower value of the applied load and hence at a lower stress. The decrease in strength with volume fraction due to particle fracture appears to outweigh the increase due to matrix strengthening. The observed reduction in yield strength parallels the observed reduction in tensile strength, suggesting that most of the particles fail below the yield strength. Particle failure would not be expected to occur during hardness testing since the loading is compressive not tensile, and an increase in hardness would therefore be expected.

The explanation given above is supported by the results obtained for the as-extruded material. In this case the matrix is not age hardened and yields and fails at lower strength. Failure occurs in this material principally by matrix failure around the particles rather than by particle fracture, indicating that matrix yielding and failure occur before the fracture strength of the particles is reached. Accordingly, the yield and tensile strengths now increase with increasing volume fraction, reflecting the inherent strengthening effect produced by particle addition.

Crawford and Griffiths [25] found that there was no change in the 0.2% proof stress or the tensile strength of their 6061 composites with increasing volume fraction of MICRAL-20^{TM}, but that the composites were stronger than the unreinforced alloy. This behaviour is in accordance with that observed in the present work, and differs from SiC-6061 composites where both of these quantities increase with increasing volume fraction. The ductility of the MICRAL-20^{TM} composites studied by Crawford and Griffiths decreased with increasing volume fraction in a similar fashion to the results reported here (Fig. 10), as well as that observed for SiC-reinforced composites. They conclude that the insensitivity of 0.2% proof stress to volume fraction is probably a result of the microplasticity induced by the reinforcement particles combined with the general inefficiency of spherical particles as reinforcements. They also state that the constant tensile strength with volume fraction appears to be a result of the constant yield stress, the decrease in ductility with increasing volume fraction and the increase in work-hardening rate with increasing volume fraction. These conclusions do not, however, appear to be supported by the behaviour of the as-extruded material observed in the present study.

5. Conclusions

1. The composites showed an accelerated aging response. However there was no systematic change in the aging response as the particle volume fraction was increased, although a progressive increase in the peak hardness was observed.

2. The composites had higher elastic moduli than the unreinforced alloy. The elastic modulus increased as particle volume fraction was increased but at a progressively decreasing rate. The decrease in the rate of stiffening with increasing particle volume fraction is attributed to an increase in the number of fractured particles present in the composites.

3. The composites had better tensile and yield strengths than the unreinforced alloy. However, there was no significant change in strength as the particle volume fraction changed. The increase in strength in the composites is attributed to an increase in the dislocation density together with an increase in the aging response. While these effects appeared to increase with increasing particle volume fraction, this increase was offset by a reduced load-carrying capability brought about by premature particle fracture.

4. The composites had lower ductility than the unreinforced alloy. The ductility decreased linearly with increasing particle volume fraction.

Acknowledgements

This work was supported by Comalco Research Centre (15 Edgars Road, Thomastown, VIC 3074, Australia) with additional funding provided through an Australian Research Council small grant. The advice and assistance of Drs M. J. Couper and K. Xia of CRC are gratefully acknowledged.

References

1. M. MANOHARAN and S. V. KAMAT, *Scripta Metall.* **25** (1991) 2121.
2. Z. Y. MA, J. LIU and C. K. YAO, *J. Mater. Sci.* **26** (1991) 1971.
3. T. S. SRIVATSAN, *Int. J. Fatigue* **17** (1995) 183.
4. D. J. LLOYD, *Int. Mater. Reviews* **39** (1994) 1.
5. C. C. PERNG, J. R. HWANG and J. L. DOONG, *Scripta Metall.* **29** (1993) 311.
6. C. GARCIA-CORDOVILLA, E. LOUIS, A. PAMIES, A. ALONSO and J. NARCISO, in Proceedings of the 9th International Conference on Composite Materials, ICCM-9, Madrid, edited by A. Miravete (1993) Vol. 1, p. 787.
7. D. L. DAVIDSON, in "Metal Matrix Composites: Mechanisms and Properties," edited by R. K. Everett and R. J. Arsenault (1991) p. 223.
8. G. L. POVICH, A. NEEDLEMAN and S. R. NUTT, *Mater. Sci. Engng* **A125** (1990) 129.
9. C. T. KIM, J. K. LEE and M. R. PLICHTA, *Metall. Trans.* **21A** (1990) 673.
10. R. J. ARSENAULT, in "Advanced Composites '93," edited by T. Chandra and A. K. Dhingra (1993) p. 19.
11. Comalco Data Sheets, Comalco Research Centre, Thomastown, Victoria, Australia (1990).
12. Y. J. YAO, G. A. EDWARDS, M. J. COUPER and G. L. DUNLOP, in Proceedings Interfaces II, IMMA, Melbourne, Australia (1993).
13. B. G. PARK, Ph.D. Thesis, University of New South Wales, Sydney, Australia , 1997.
14. M. J. COUPER, N. SETARGEW, A. H. A. CLAYTON, R. TARR and S. BANDYOPADHYAY, in Proceedings of the Conference on Materials United in the Service of Man, edited by R. D. Davies and D. I. Hatcher (IMMA/WTIA, Perth, Australia, 1990) Vol. 1, p. 1.

15. H. J. RACK and R. W. KRENZER, *Metall. Trans.* **8A** (1977) 355.
16. "Metals Handbook," Vol. 2, 10th ed. (American Society for Metals, Metals Park, OH, 1990).
17. J. M. PAPAZIAN, *Metall. Trans.* **19A** (1988) 2945.
18. S. DIONNE and S. H. J. LO, in Proceedings of the 8th International Conference on Composite Materials, ICCM-VIII, Honolulu, Hawaii, 1991, edited by S. W. Tsai and G. S. Springer, p. 21-B.
19. Z. HASHIN and S. SHTRIKMAN, *J. Mech. Phys. Solids* **11** (1963) 127.
20. A. Z. REUSS, *Angew. Math. Mech.* **9** (1929) 49.
21. X. GE and S. SCHMAUDER, *Mater. Sci. Engng.* **A168** (1993) 93.
22. J. C. HALPIN, in "Primer on Composite Materials: Analysis" (Technomic Publications, Lancaster, PA, 1984).
23. S. F. CORBIN and D. S. WILKINSON, *Acta Metall. Mater.* **42** (1994) 1311.
24. S. ELOMARI, R. BOUKHILI, M. D. SKIBO and J. MASOUNAVE, in Proceedings of the 10th International Conference on Composite Materials, ICCM-10, 1995, p. II-369.
25. B. R. CRAWFORD and J. R. GRIFFITHS, in Proceedings of Materials 98, Wollongong, July 1998, edited by M. Ferry (Institute of Materials Engineering Australasia, 1998) p. 723.
26. N. V. RAVI KUMAR and E. S. DWARAKADASA, *J. Mater. Sci.* **29** (1994) 1533.
27. S. DIONNE, M. R. KRISHNADEV and R. BOUCHARD, in "Metal and Ceramic Matrix Composites: Processing, Modeling & Mechanical Behavior," edited by R. B. Bhagat, A. H. Clauer, P. Kumar and A. M. Ritter (TMS, 1990) p. 243.

Received 17 July
and accepted 3 November 2000